Published in final edited form as:
Mol Cell Neurosci. 2012 November ; 51(3-4): 112–126. doi:10.1016/j.mcn.2012.08.014.

Distinct contributions of *Galgt1* and *Galgt2* to carbohydrate expression and function at the mouse neuromuscular junction

Neha Singhal[#], **Rui Xu**[^], and **Paul T. Martin**[^,+,*]

[^]Center for Gene Therapy, The Research Institute at Nationwide Children's Hospital, 700 Childrens Drive Columbus, OH 43205

[+]Department of Pediatrics, Department of Physiology and Cell Biology, The Ohio State University College of Medicine 700 Childrens Drive Columbus, OH 43205

[#]Integrated Biomedical Sciences Graduate Program The Ohio State University College of Medicine, 700 Childrens Drive Columbus, OH 43205

Abstract

At the mammalian neuromuscular junction (NMJ), the CT (cytotoxic T cell) carbohydrate antigen [GalNAcβ1,4[Neu5Ac/Gcα2,3]Galβ1,4GlcNAc-] is a uniquely synaptic cell surface carbohydrate present in both the presynaptic and postsynaptic membrane. Here we show that Galgt1, which synthesizes the β1,4GalNAc linkage of the CT carbohydrate on gangliosides, is required for presynaptic expression of the CT carbohydrate at the NMJ, while Galgt2, which can synthesize the β1,4GalNAc of the CT carbohydrate on glycoproteins, is required for postsynaptic expression. Proper postsynaptic localization of the CT carbohydrate also required muscle expression of dystroglycan, a known muscle substrate for Galgt2. Transgenic overexpression of Galgt2 in skeletal myofibers altered the expression of synaptic muscle proteins and altered neuromuscular topography, which was partially NCAM-dependent, while an increase in postsynaptic AChR-rich domains was observed in both neuron- and skeletal muscle-specific Galgt2 transgenic mice. By contrast, overexpression of Galgt1 in muscle did not allow for increased expression of CT carbohydrate on the sarcolemmal membrane and instead caused muscle histopathology. Loss of Galgt2 increased intracellular accumulation of acetylcholine receptors and acetylcholinesterase within skeletal myofibers, suggesting an additional role for Galgt2 in neuromuscular stability. These experiments demonstrate that Galgt1 and Galgt2 contribute in distinct ways to the expression and function of synaptic βGalNAc-containing carbohydrates at the NMJ.

Keywords

Neuromuscular junction; synapse; ganglioside; dystroglycan; muscular dystrophy; acetylcholine receptor

[*]Author for Correspondence Phone (614) 722-4072; FAX (614) 722-5893; Paul.Martin@nationwidechildrens.org.

Introduction

Synapses contain large collections of proteins and lipids linked together to form specialized complexes within the pre- and postsynaptic cellular membranes and the synaptic cleft, and cell surface carbohydrates can play important roles in defining the localization and function of such synaptic molecules(Dani and Broadie, 2012; Martin, 2002, 2003a, b; Martin and Freeze, 2003; Rushton et al., 2012). At the vertebrate neuromuscular junction (NMJ), the synaptic connection made between the nerve terminal of motor neurons and skeletal myofibers, there are several carbohydrates known that may participate in aspects of synaptic development and function(Dani and Broadie, 2012; Hoyte et al., 2002; Jenniskens et al., 2000; Martin et al., 1999; Sanes and Cheney, 1982; Scott et al., 1988; Singhal and Martin, 2011). One such structure is the Cytotoxic T cell (CT) carbohydrate, GalNAcβ1,4[Neu5Ac/Gcα2,3]Galβ1,4GlcNAc-R(Conzelmann and Lefrancois, 1988). Antibodies that recognize this structure cross-react with the human SDA and CAD blood group antigens(Conzelmann and Lefrancois, 1988; Montiel et al., 2003). The localized muscle expression of the CT carbohydrate at the NMJ results from the presence of β1,4-linked N-acetylgalactosamine (βGalNAc);Terminal βGalNAc structures are confined to the NMJ in mammals ranging from mice, rats, hamsters, guinea pigs, dogs and cats to monkeys and humans, and they are also localized to the NMJ in goldfish, frogs, chickens, axolotls, snakes and lampreys (Martin, 2003b; Sanes and Cheney, 1982; Scott et al., 1988). The form of sialic acid on the CT carbohydrate helps to contribute to pre- vs. post-synaptic specificity; CT2, a monoclonal anti-CT antibody that recognizes GalNAcβ1,4 [Neu5Gcα2,3]Galβ1,4GlcNAc-R, stains primarily the postsynaptic membrane, while CT1, which recognizes GalNAcβ1,4 [Neu5Acα2,3]Galβ1,4GlcNAc-R, primarily stains the presynaptic membrane(Hoyte et al., 2002; Martin et al., 1999).

The synaptic βGalNAc portion the CT carbohydrate is synthesized by Galgt2, a β1,4GalNAc transferase whose expression is also highly confined to synaptic regions in skeletal myofibers(Smith and Lowe, 1994; Xia et al., 2002). Galgt2 is known to glycosylate only a small set of glycoproteins, including α dystroglycan in skeletal muscle and agrin in mammalian cell lines, as well as a non-GM2/GD2 glycolipid in skeletal muscle(Kawamura et al., 2005; Lefrancois and Bevan, 1985; Nguyen et al., 2002; Xia et al., 2002; Xia and Martin, 2002; Xu et al., 2007; Yoon et al., 2009). By contrast, Galgt1, also called the GM2/GD2 synthase, is a β1,4GalNAc transferase specific for ganglioside glycolipid substrates(Takamiya et al., 1996). As such, Galgt1 is required for the biosynthesis of complex gangliosides(Takamiya et al., 1996). Because GM2 (GalNAcβ1,4 [Neu5Ac/Gcα2,3]Galβ1,4Glc-Ceramide) and GD2 gangliosides, like the CT carbohydrates that occur on proteins, are localized to the NMJ(Martin et al., 1999), there is the potential for redundancy between Galgt1 and Galgt2 with regard to synaptic glycan biosynthesis and function. Here, we use genetic methods in the mouse to dissect the relative contributions of Galgt1 and Galgt2 to the synthesis of synaptic CT carbohydrates at the NMJ and determine the relative impact of their overexpression and loss of expression on neuromuscular development.

Results

Galgt1 and Galgt2 contribute in unique ways to the formation of synaptic CT carbohydrates at the neuromuscular junction

We had previously made affinity purified polyclonal antibodies to Galgt2 and demonstrated that Galgt2 protein expression is highly concentrated at the neuromuscular junction (NMJ) in skeletal muscle(Hoyte et al., 2002; Xia et al., 2002). Here, we made affinity purified antibodies to Galgt1 and showed that Galgt1 protein is also concentrated in neuromuscular regions of adult skeletal muscles (Fig. 1). Galgt1 expression was highly co-localized with

postsynaptic nicotinic acetylcholine receptors (AChRs), which were stained with α bungarotoxin, as was GM1, a *Galgt1*-dependent ganglioside. GM1 staining was also present elsewhere within skeletal muscle sections, including capillaries. Both Galgt1 and GM1 staining were absent from NMJs in *Galgt1*$^{-/-}$ skeletal muscle, showing the specificity of the antibodies for their intended targets (Fig. 1). Thus Galgt1, like Galgt2, likely synthesizes βGalNAc-linked carbohydrate antigens locally at the synapse due to its concentration in synaptic regions of skeletal myofibers.

Because both Galgt1 and Galgt2 are concentrated in postsynaptic regions of skeletal muscles, we took a genetic approach to understand their contributions to the synaptic expression of pre- and postsynaptic CT carbohydrates. To do this, we analyzed CT1 and CT2 staining at the NMJ in mice containing genetic deletions of *Galgt1* (*Galgt1*$^{-/-}$), *Galgt2* (*Galgt2*$^{-/-}$) or both *Galgt1* and *Galgt2* (*Galgt1*$^{-/-}$*Galgt2*$^{-/-}$). All three genetic deletion strains were compared to wild type (WT) animals maintained on a similarly pure genetic background (C57Bl/6). In WT muscle, CT1 expression was often offset from α bungarotoxin staining, consistent with presynaptic localization, while CT2 expression was more coincident with postsynaptic AChR expression, as expected of postsynaptic localization, much as we had previously observed(Martin et al., 1999) (Fig. 2). In *Galgt1*$^{-/-}$ muscle, CT1 expression was lost, while CT2 expression was maintained on and near the postsynaptic membrane. Some extrasynaptic expression of CT2 was also present in *Galgt1*$^{-/-}$ muscle that was not obvious in WT muscle. This staining may reflect altered CT expression due to loss of *Galgt1*, but CT2 staining was nevertheless still present at NMJs. In *Galgt2*$^{-/-}$ muscles, CT1 expression remained present at NMJs in a presynaptic pattern, while postsynaptic CT2 expression was lost (Fig. 2). Intracellular and juxtamembrane puncta of CT1 immunostaining were also present in *Galgt2*$^{-/-}$ muscles. In *Galgt1*$^{-/-}$*Galgt2*$^{-/-}$ muscle, staining of both CT1 and CT2 were absent at the NMJ (Fig. 2). Only non-specific staining of large blood vessels was evident in these muscles. These data demonstrate that *Galgt1* and *Galgt2* both contribute to synaptic expression of the CT carbohydrates, with *Galgt1* being required for proper presynaptic expression and *Galgt2* for proper postsynaptic expression.

Dystroglycan is required for postsynaptic localization of CT2 at the neuromuscular junction

Overexpression of Galgt2 in skeletal muscle leads to increased glycosylation of α dystroglycan with the CT2 carbohydrate, and α dystroglycan is the predominant glycoprotein evident in *Galgt2* transgenic muscles (Nguyen et al., 2002; Xia et al., 2002). Dystroglycan (both the α and β chain) is present along the entirety of the sarcolemmal membrane, but is also concentrated in the postsynaptic membrane at the NMJ(Matsumura et al., 1992), where Galgt2 and CT2 are also normally localized(Martin et al., 1999; Xia et al., 2002). Because dystroglycan is an essential gene in mice(Williamson et al., 1997) and because deletion of dystroglycan in skeletal muscles causes muscular dystrophy(Cohn et al., 2002), we utilized a unique Pax3-driven Cre transgenic line (P3Pro-Cre) to delete a floxed allele of dystroglycan (*Dag1*$^{loxP/loxP}$) specifically in hindlimb skeletal muscles(Jarad and Miner, 2009).

Dystroglycan was expressed normally in forelimb muscles such as the triceps and biceps of P3ProCre*Dag1*$^{loxP/loxP}$ mice (Fig. 3). By contrast, P3Pro-Cre*Dag1*$^{loxP/loxP}$ mice showed no expression of α or β dystroglycan in skeletal myofibers of hindlimb muscles, including the gastrocnemius and tibialis anterior (TA) (Fig. 3). Dystroglycan was also absent from NMJs in these muscles, as evidenced by lack of co-staining with rhodamine α bungarotoxin (Fig. 3). Because deletion of dystroglycan causes muscular dystrophy, there was expression of dystroglycan in some mononuclear cells within the muscle, most likely macrophages, however expression was absent in skeletal myofibers.

In the gastrocnemius muscle of P3Pro-Cre*Dag1*$^{loxP/loxP}$ mice, CT1 staining was still present at the NMJ, while CT2 staining was reduced or absent (Fig. 4). Instead, CT2 staining primarily was present in intracellular puncta, with occasional patches of sarcolemmal membrane staining removed from postsynaptic AChRs. All muscles also showed some CT carbohydrate staining of intramuscular capillaries, as previously described (Martin et al., 1999)(Fig. 4). CT2 staining was, however, coincident with AChRs in hindlimb muscles taken from wild type, P3Pro-Cre or *Dag1*^{loxPloxP} mice, where dystroglycan is not deleted (Fig. 4). These data suggest that dystroglycan is required for the proper localization of postsynaptic CT2 carbohydrate at the NMJ.

Phenotypes of Galgt2 overexpression in skeletal muscle and neurons

Even though *Galgt2* was not required for presynaptic expression of CT1 (Fig. 2), *Galgt2* expression in motor neurons could still contribute to the expression of CT carbohydrates in the postsynaptic membrane or in the synaptic cleft via secretion of CT-glycosylated proteins from the motor nerve terminal. To test this, we made four independent lines of *Galgt2* transgenic mice (nCT) using the “neuron-specific” elements of the Thy1 promoter (Thy1.2) (Fig. 5). All four nCT lines showed no overt phenotypes and lived to beyond one year of age. An N-terminal FLAG epitope tag was placed before the Galgt2 protein to discriminate transgenic protein from endogenous protein. The presence of this tag did not affect Galgt2 enzyme activity in a number of different assays ((Xia et al., 2002; Yoon et al., 2009) and not shown). Immunoblots of whole tissue SDS protein extracts showed that nCT mice overexpressed transgenic Galgt2 protein most highly in retina, brain and spinal cord and did not express detectable transgenic protein in skeletal muscle, heart, thymus, spleen, pancreas, liver or intestine (Fig. 5A). Some expression, however, was detected in lung, testes, and kidney. Thus, use of the Thy1.2 promoter did not yield completely neuron-specific expression. In addition, some cleavage of the FLAG tag occurred in some tissues, yielding a 10kDa fragment in addition to the native 68kDa full-length protein.

We analyzed changes in CT glycosylation in four different ways. First, we stained brain and spinal cord with *Wisteria floribunda* agglutinin (WFA), a βGalNAc binding lectin, to see overall increases in βGalNAc. While some WFA was present in many brain regions of nCT mice, we observed high increases in the hippocampus (particularly the dentate gyrus), cerebellum (particularly the Purkinje cell layer), olfactory bulb, anterior pituitary, cortex, and ventral spinal cord (which includes motor neurons) (Fig. 5B). Second, we stained brain sections with CT1 antibody to visualize increases specifically in the CT carbohydrate. Though more muted than WFA, we observed increased axonal staining throughout the brain, including in the ventral hippocampal commissure, the dentate gyrus, the anterior pituitary and the accumbens nucleus (Fig. 5C). Third, we analyzed whole brain and spinal cord SDS protein lysates for changes in protein glycosylation by CT1 immunoblotting. We observed increased expression of CT antigen on only several proteins, with a predominantly increased band at 400kDa (Fig. 5D). Fourth, we used lectin precipitation of non-ionic detergent brain lysates to identify glycoproteins with increased βGalNAc in nCT brain, much as we had done previously to identify α dystroglycan as a target of Galgt2 in skeletal muscle(Nguyen et al., 2002; Xia et al., 2002). We did not identify α dystroglycan by immunoblotting of WFA precipitates of nCT brain, nor did we identify agrin, a 400kDa protein that can be glycosylated with CT carbohydrate in cultured cells overexpressing *Galgt2* (not shown)(Xia and Martin, 2002). We did, however, identify reelin, a 400kDa protein, specifically in WFA precipitates from nCT brain (Fig. 5E).

We next compared the molecular and cellular changes resulting from *Galgt2* overexpression in the postsynaptic or presynaptic cell (Figs. 6-8). For muscle-specific transgenic mice (mCT), immunostaining for Galgt2 was present in most skeletal myofibers (Fig. 6). By contrast, wild type (Wt) and neuron-specific transgenic (nCT) muscles only showed Galgt2

immunostaining at the NMJ (arrows in Fig. 6). Similarly, CT carbohydrate immunostaining was present in the sarcolemmal membranes of all mCT myofibers, while Wt and nCT muscles showed CT immunostaining at NMJs and capillaries, much as previously reported(Martin et al., 1999). nCT muscles also showed intracellular accumulations of CT carbohydrate in skeletal myofibers (arrowheads in Fig. 6), even though the *Galgt2* transgene is not overexpressed in nCT muscles(Fig. 5A). These data suggest that Galgt2 expression in motor neurons may stimulate the uptake of presynaptic CT carbohydrate into skeletal muscle. Several normally synaptic basal lamina proteins (laminin α4 and laminin α5) and the muscle membrane protein NCAM (neural cell adhesion molecule) were also overexpressed along the sarcolemmal membrane in mCT mice, much as observed previously(Xia et al., 2002), but this overexpression was not observed in nCT muscle (Fig. 6). Thus, only muscle overexpression of Galgt2 causes upregulation of these normally synaptic muscle proteins.

We had previously shown that mCT muscles have an expanded endplate band, the region of muscle normally innervated motor neurons(Xia et al., 2002). In addition, mCT muscles show aberrant migration and sprouting of motor axons as well as increased numbers of AChR-rich postsynaptic domains(Xia et al., 2002). Here, we compared mCT muscles to nCT muscles for these measures (Figs. 7 and 8). α bungarotoxin staining of whole mount preparations of diaphragm showed an average 3-fold increase in the distribution of postsynaptic AChRs along myofibers in the diaphragm of mCT mice compared to WT or nCT (Figs. 7A, 8A, 8B). Because transgenic overexpression of NCAM in skeletal muscle stimulates axonal sprouting of motor axons(Walsh et al., 2000), and because NCAM is overexpressed in extrasynaptic regions of mCT myofibers (Fig. 6), we assessed the role of NCAM more directly by crossing mCT mice to NCAM-deficient animals (*Ncam*$^{-/-}$)(Cremer et al., 1994). Deletion of *Ncam* from mCT mice reduced the expansion of the endplate band region in the diaphragm by half (Fig. 8C), suggesting a role for NCAM in mCT endplate band expansion. Non-transgenic *Ncam*$^{-/-}$ mice showed no change in endplate band topography in the diaphragm (not shown), consistent with the confinement of NCAM to synaptic regions in adult wild type muscle(Covault and Sanes, 1986).

Postsynaptic AChR expression in mCT mice was more disorganized relative to WT and nCT, with AChR aggregates being smaller (Fig. 7A). In addition, mCT NMJs had an average 100% reduction in cross-sectional diameter relative to Wt, consistent with the reduced size of mCT myofibers(Xia et al., 2002) (Figs. 7A and 8D). Additionally, both mCT and nCT muscles frequently had multiple AChR-rich domains along individual skeletal myofibers (Fig. 7A and 8E). The presence of multiple AChR-rich postsynaptic domains along myofibers was roughly an order of magnitude higher in both mCT and nCT muscles at 2 months of age relative to wild type, both the diaphragm and the tibialis anterior muscle (Figs. 8E). nCT and mCT mice both demonstrated this phenotype, even though changes in synaptic topography were not evident in nCT muscles.

To more carefully assess the contributions of individual motor neurons to these phenotypes, we crossed nCT mice to Thy1-YFP-H transgenic mice(Feng et al., 2000). Thy1-YFP-H transgenic mice overexpress YFP only in a small number of motor neurons due to the site of transgene insertion, allowing one to visualize and follow the innervation patterns of single neurons more easily. YFP-positive neurons in nCT/YFP-H diaphragm muscle showed a pattern of innervation consistent with an unchanged endplate band and normal pre-and postsynaptic alignment (Fig. 7B). Staining of teased myofibers from nCT/YFP-H mice showed multiple AChR domains innervated by YFP-labeled motor neurons (Fig. 7C). Some YFP-labeled motor neurons showed axonal sprouting within individual AChR domains (NMJ 4 in Fig. 7C).

Transgenic overexpression of Galgt1 in skeletal muscle

To assess the effects of *Galgt1* overexpression in skeletal muscle, we infected muscles with AAV1-CMV-*Galgt1*, an adeno-associated virus (AAV) vector designed to overexpress the *Galgt1* cDNA. We injected AAV-CMV-*Galgt1* into wild type Gastroc and TA muscles at one week of age and analyzed Galgt1 protein and CT carbohydrate antigen expression at 6 or 12 weeks post-infection. Single stranded AAV vectors typically take 3 weeks to reach maximal gene expression in skeletal muscle and largely only infect skeletal myofibers when injected in this manner (Xiao et al., 1998; Xu et al., 2007). By 6 weeks post-infection, we identified large numbers of myofibers overexpressing Galgt1 protein in an intracellular pattern consistent with its normal localization to the Golgi apparatus (Fig. 9A). Unlike overexpression of *Galgt2*, however, which leads to uniform distribution of CT carbohydrate along the sarcolemmal membrane(Nguyen et al., 2002; Xia et al., 2002), *Galgt1* overexpression only led to accumulation of intensely stained intracellular and juxtamembrane punta using anti-CT carbohydrate antibodies (Fig. 9A). By contrast, overexpression of Galgt1 in various tumor cell lines lead to cell surface glycosylation of glycolipids (not shown). By 6 weeks of age, *Galgt1* overexpression caused a reduction skeletal muscle growth; Average myofiber diameters were significantly reduced in AAV1-CMV-*Galgt1*-infected muscles (Fig. 9B, by 22% in the Gastroc ($P<0.001$) and by 17% in the TA ($P<0.05$)). This reduction was retained at 12 weeks post-infection (16% in Gastroc, $P<0.01$ and 21% in TA, $P<0.05$). By 12 weeks post-infection, *Galgt1* overexpression had induced a significant increase in the number of myofibers with central nuclei (Fig. 9C) and in the coefficient of variance in myofiber diameter (Fig. 9D). Both of these measures are indicative of increased muscle histopathology. Thus, *Galgt1* overexpression in muscle was unable to induce significant membrane expression of the CT carbohydrate and instead stimulated intracellular CT accumulation associated with reduced muscle growth and increased muscle histopathology. One additional unusual feature of *Galgt1* muscle overexpression was the accumulation of mononuclear cells near large blood vessels (Fig. 9B, lower left panels), which was noted on multiple occasions.

A neuromuscular phenotype in adult Galgt2$^{-/-}$ skeletal muscles

Galgt2-deficient mice (*Galgt2*$^{-/-}$) have no overt neuromuscular phenotypes such as weakness or spasticity that would suggest dramatic alterations in NMJ biology. Analysis of *Galgt2*$^{-/-}$ muscles, however, showed increased accumulation of α bungarotoxin staining in intracellular microaggregates by 3 months of age (Fig. 10). Staining for synaptic α dystroglycan and synaptic dystroglycan-associated proteins (utrophin) and ligands (laminin α5, agrin) showed no change in *Galgt2*$^{-/-}$ muscle relative to wild type and no appreciable intracellular accumulations (Fig. 10A,C). Staining of laminin α2 and α sarcoglycan, which are present in both extrasynaptic and synaptic regions, was also normal (Fig. 10A,C). In muscles from mice of 3 months or older, intracellular micro-aggregates of AChRs were present, and these co-localized with acetylcholinesterase (AChE), a βGalNAc-containing synaptic cleft glycoprotein (Fig. 10B,C) (Scott et al., 1988). 3 month-old *Galgt2*$^{-/-}$ gastrocnemius muscle had an order of magnitude increase in intramuscular AChR and AChE microaggregates compared to age-matched wild type muscle (Fig. 10C). The cross sectional area of the NMJ and of skeletal myofibers, however, was unchanged in *Galgt2*$^{-/-}$ animals (Fig. 10D and E). While a subtle phenotype, these studies demonstrate that Galgt2-deficiency alters the patterning of synaptic AChR and AChE expression with age and may reflect changed synaptic protein stability.

To assess what intracellular compartments AChR microaggregates might be in, we co-stained muscle from 3 month-old *Galgt2*$^{-/-}$ mice for AChRs and markers for the endoplasmic reticulum (ER, calnexin), trans-Golgi (TGN38), lysozome (Lamp1) and endosome (clathrin heavy chain) (Fig. 11). AChR microaggregates did not co-stain with Lamp1 or calnexin,

suggesting no trapping of intracellular AChRs in the ER or lysosome. A few AChR microaggregates were co-localized with the trans-Golgi marker TGN38, but many more co-stained with clathrin heavy chain, demonstrating increased expression of AChRs in endosomes. No such increase in intracellular aggregates was observed in *Galgt1*$^{-/-}$ muscles (not shown), consistent with previously published data(Bullens et al., 2002). Thus, *Galgt2*-deficiency appears to alter AChR dynamics such that AChRs are either increasingly internalized via endosomes or trapped prior to secretion in the trans Golgi and endosomes.

Discussion

The fact that the same carbohydrate structure can be made by different glycosyltransferases on different classes of molecules significantly complicates the understanding of carbohydrate function. This challenge is made even more difficult with regard to understanding the roles of carbohydrates at synapses, because glycoproteins and glycolipids enriched there may emanate from multiple cellular elements. For the neuromuscular junction (NMJ), these cellular players include the presynaptic motor neuron, the postsynaptic skeletal myofiber, and the pre-synaptic non-myelinating Schwann cell(Sanes and Lichtman, 2001). As a group, these cells contribute to the synaptic concentration of β-linked terminal N-acetyl-D-galactosamine (βGalNAc) in species ranging from lamprey to human(Hoyte et al., 2002; Martin et al., 1999; Sanes and Cheney, 1982; Scott et al., 1988).

Here we describe the concentration of two β1,4GalNAc glycosyltransferases, *Galgt1* and *Galgt2*, in synaptic regions of mouse skeletal myofibers. The postsynaptic concentration of both enzymes is consistent with the finding that antibodies to the CT carbohydrate, which can reflect βGalNAc on glycoproteins and/or gangliosides, stain the postsynaptic muscle membrane(Martin et al., 1999). Through analysis of mice lacking *Galgt1* and/or *Galgt2* by gene deletion, we show that *Galgt1* is required for presynaptic expression of the CT carbohydrates and *Galgt2* for postsynaptic expression. This does not discount the possibility that other βGalNAc transferases, for example those involved in the biosynthesis of chondroitin sulfate glycosaminoglycans, may also be present and contribute to synaptic glycosylation in ways we have not detected here. In addition, *Galgt1*$^{-/-}$ muscle did show some extrasynaptic CT2 expression. As such, postsynaptic gangliosides may have a role, though not absolute, in facilitating or consolidating postsynaptic CT carbohydrate expression. A simplistic model emerging from this genetic data, however, is that presynaptic CT carbohydrates occur predominantly on gangliosides requiring *Galgt1*, while postsynaptic CT carbohydrates occur predominantly on glycoproteins or glycolipids requiring *Galgt2*. Here it is important to note that overexpression of *Galgt2* in skeletal muscle leads to increased CT glycosylation of α dystroglycan as well as one non-GM2/GD2 glycolipid (Nguyen et al., 2002; Xia et al., 2002; Xu et al., 2007). Thus, deletion of Galgt2 may impact non-ganglioside glycolipid glycosylation as well as glycoprotein glycosylation.

We also describe here a role for dystroglycan in localizing the CT carbohydrates at the NMJ. While we cannot yet ascertain the relative contributions of particular Galgt2 substrates to overall postsynaptic CT carbohydrate expression, elimination of dystroglycan from skeletal myofibers led to a failure of CT carbohydrate to localize properly to the postsynaptic muscle membrane. Thus, dystroglycan is required for the proper postsynaptic expression of the CT carbohydrate and may therefore be a synaptic organizer of Galgt2 activity and perhaps also a synaptic Galgt2 substrate. α dystroglycan is clearly a substrate for Galgt2 *in vitro*(Yoon et al., 2009). Overexpression of Galgt1 in skeletal muscle, by contrast, did not allow for membrane expression of CT carbohydrate and instead caused muscle pathology. This may be due to a lack of ganglioside substrates for Galgt1 in the extrasynaptic muscle membrane or an inability of GM2 or GD2, once made, to maintain membrane expression. Regardless, the presence of increased CT carbohydrate staining in intracellular puncta after Galgt1

overexpression suggests Galgt1 is unable to accomplish the dramatic membrane overexpression of CT carbohydrate that can occur with Galgt2, which can, in turn, alter the expression of synaptic muscle molecules and inhibit disease in at least three mouse models of muscular dystrophy (Martin et al., 2009; Nguyen et al., 2002; Xia et al., 2002; Xu et al., 2007; Xu et al., 2009).

We have learned several additional things by comparing transgenic overexpression of Galgt2 in skeletal myofibers and in neurons. Overexpression of Galgt2 in neurons led to the increased expression of likely internalized CT carbohydrate in skeletal myofibers, suggesting Galgt2 expression in motor neurons may contribute to synaptic cleft CT carbohydrate expression via secretion of CT-expressing glycoproteins or glycolipids. One such protein may be reelin, which shows increased βGalNAc in nCT brain. Such CT-glycosylated glycoproteins or glycolipids may be involved in the phenotype we identified of increased AChR-rich postsynaptic domains in nCT muscle. Muscle-specific *Galgt2* transgenic mice (mCT) also showed such changes, but with dramatically more pronounced effects on axonal migration and endplate bandwidth. mCT muscles also showed ectopic overexpression of normally synaptic muscle extracellular matrix and membrane proteins, including NCAM. Expansion of the endplate band to its fullest extent in mCT mice required the expression of NCAM, suggesting that ectopic overexpression of NCAM, in part, drives the altered migration of motor axons in mCT muscles. NCAM can have terminal β1,4-linked GalNAc by virtue of carbohydrates present on its GPI-linked anchor(Mukasa et al., 1995) and overexpression of GPI-linked NCAM in skeletal muscle stimulates sprouting of motor axons(Walsh et al., 2000). Axonal sprouting could also be caused by the ectopic expression of polysialic acid, which also can be present on NCAM(Rutishauser and Landmesser, 1996).

Cell surface carbohydrates also serve as receptors for infectious agents, particularly viruses and bacteria, and exhibit altered tissue expression during the course of evolution(Varki, 2006). Given that, the phylogenetic conservation of βGalNAc at the vertebrate NMJ suggests the carbohydrate has an important function. Elimination of both *Galgt1* and *Galgt2* in mice, however, argues to the contrary, as these animals move and breathe normally for many months. Previous studies have shown that deletion of *Galgt1* in mice leads to Wallerian degeneration of motor axons in aging animals(Pan et al., 2005; Sheikh et al., 1999). This only occurs once *Galgt1*$^{-/-}$ mice are well into adulthood(Pan et al., 2005; Sheikh et al., 1999). Prior to that, NMJs in *Galgt1*-deleted mice show no obvious change in NMJ structure or function, aside from losing pre-synaptic binding to botulinum neurotoxin(Bullens et al., 2002). All of our studies have focused on early postnatal development, up to 3 months, so as to bypass issues that might result from loss of *Galgt1* in aging animals. In this early time period, loss of *Galgt2* causes apparent neuromuscular instability, as evidenced by increased expression of acetylcholine receptors within skeletal myofibers, some in clathrin-coated endosomes. Previous studies suggest a model as to why this would occur. Galgt2 overexpression causes increased CT glycosylation of α dystroglycan(Nguyen et al., 2002; Xia et al., 2002), stimulates ectopic overexpression of synaptic ECM proteins(Xia and Martin, 2002; Xu et al., 2007)) and increases ECM binding to α dystroglycan(Yoon et al., 2009). In addition, synaptic laminins, agrin, and dystroglycan are all required for proper neuromuscular development, stability and/or maturation(Burgess et al., 1999; Cote et al., 1999; Gautam et al., 1996; Misgeld et al., 2005; Nishimune et al., 2008). Given this, it certainly seems plausible that loss of *Galgt2* in mice inhibits synaptic CT glycosylation of α dystroglycan, thereby destabilizing synaptic ECM binding and synaptic AChR and AChE localization. Future work will be required to test this theory. AChE is also glycosylated with βGalNAc on its synaptic ColQ subunit in mouse skeletal muscle(Scott et al., 1988). As synaptic AChE expression in intracellular aggregates is also increased in *Galgt2*$^{-/-}$ mice, loss of βGalNAc glycosylation on AChE could also mediate such changes.

Materials and Methods

Materials

Antibody to reelin (sc-7741) was obtained from Santa Cruz Biotechnology (Santa Cruz, CA). Antibodies to neurofilament 200 (clone N52) and the FLAG peptide (M2) were obtained from Sigma (St. Louis, MO). Antibody to synaptophysin (SY38) was obtained from Boehringer Mannheim (Indianapolis, IN). Antibody to laminin α2 was obtained from Alexis Biochemicals (San Diego, CA). Antibody to α dystroglycan (IIH6) was obtained from Upstate Biotechnology (Lake Placid, NY). Antibodies to utrophin (DRP2), dystrophin (DYS1), β dystroglycan (43DAG) and α sarcoglycan (a-SARC) were obtained from Nova Castra (Newcastle-Upon-Tyne, UK). Antibodies to NCAM, laminin α4 and laminin α5 were gifts from Joshua Sanes (Harvard University), Bruce Patton (Oregon Health Sciences University) and Jeffery Miner (Washington University), respectively. Antibody to agrin was a gift from Michael Ferns (UC Davis). Antibody to acetylcholinesterase was a gift from Palmer Taylor (UC San Diego). Additional antibody to laminin α2 was from Sigma-Aldrich (L0663), as were antibodies to calnexin (C4731) and Lamp1 (L1418). Antibody to clathrin heavy chain was from Cell Signaling (2410) and antibody to TGN38 was from Serotoc (AHP499G). Rhodamine-α-bungarotoxin was purchased from Molecular Probes (Eugene, OR). *Wisteria floribunda* agglutinin (WFA) and Wheat Germ agglutinin (WGA) coupled to agarose were purchased from EY Laboratories (San Mateo, CA). Secondary antibodies conjugated to fluorophores were purchased from Jackson ImmunoResearch (West Grove, PA). Antibodies to CT1, CT2 and Galgt2 were produced in our lab as previously described(Martin et al., 1999; Xia et al., 2002). Rabbit polyclonal antibody to Galgt1 peptide (CQVRAVDLTKAFDAEE) was made by immunizing rabbits with KLH-conjugated peptide, after which antibody was purified over peptide-conjugated resin as previously described(Xia et al., 2002).

Mice

Transgenic mice made to overexpress the CT GalNAc transferase (*Galgt2*) in their skeletal muscles (mCT) have been previously described(Nguyen et al., 2002; Xia et al., 2002). These mice were bred to NCAM-deficient mice ($Ncam^{-/-}$, from Jackson Labs (line 002405) (Cremer et al., 1994)) to make mCT$Ncam^{+/-}$ and mCT$Ncam^{-/-}$ animals. To make mice that expressed the CT GalNAc transferase in neurons (nCT), a cDNA encoding the mouse *Galgt2* cDNA was ligated into the XhoI site in the pThy 1.2 cassette, a vector containing neuron-specific promoter elements and introns from the *Thy1* gene(Caroni, 1997). The cDNA for *Galgt2* contained a FLAG epitope tag at its N-terminus to allow the detection of transgenic protein. DNA was linearized by digestion with PvuI and partial digestion with EcoR1, purified, and injected into fertilized oocytes as previously described(Xia et al., 2002). Injections were done at the UCSD Cancer Center Mouse Core Facility (La Jolla, CA). Transgene integration was confirmed by PCR analysis and subsequent Southern blot. Oligonucleotides used to confirm transgene integration were 5'TCTGAGTGGCAAAGGACCTTAGG(forward) and 5'TGCCTGTCTTCTGGCATTCAC(reverse). Four lines of pThy1.2-*Galgt2* transgenic mice (5129, 5115, 5131, and 5144) were generated. All findings were confirmed in at least two lines of transgenic mice. YFP-H mice (line 003782) originally described by Sanes and colleagues (Feng et al., 2000) were obtained from Jackson laboratories (Bar Harbor, ME). YFP-H mice were bred to nCT mice to create nCT/YFP-H double transgenic lines. YFP-H mice were genotyped using previously described methods (Feng et al., 2000).

Mice lacking Galgt2 ($Galgt2^{-/-}$) were made by John Lowe (Genentech, South San Francisco CA) and mice lacking Galgt1 ($Galgt1^{-/-}$) were obtained from the Consortium for Functional Glycomics. Double mutant mice ($Galgt1^{-/-}Galgt2^{-/-}$) were made by interbreeding the two

lines on a pure C57Bl/6 genetic background. Mice lacking dystroglycan (*Dag1*) in caudal but not rostral muscles(Jarad and Miner, 2009) were made by breeding P3Pro-*Cre* transgenic mice (originally made by Epstein and colleagues, U. Pennsylvania(Li et al., 2000)) to *Dag1*$^{loxP/loxP}$ mice (originally made by Campbell and colleagues, U. Iowa(Cohn et al., 2002; Moore et al., 2002)) to create P3Pro-Cre*Dag1*$^{loxP/loxP}$ animals.

Histology

Whole mounts of diaphragm were done as previously described(Xia et al., 2002). For immunostaining of muscle sections, mouse muscles were snap frozen in liquid nitrogen-cooled isopentane and sectioned at 8-10μm on a cryostat. For analysis of brains and spinal cords, mice were exsanguinated under anesthetic and fixed in 4% paraformaldehyde. Tissues were dehydrated in sucrose, mounted in OCT, and frozen in dry ice-cooled isopentane. All tissues were sectioned (at 10μm for brain and spinal cord and at 8 μm for all other tissues) on a cryostat and mounted on gelatin-coated glass slides. Tissue sections were blocked in phosphobuffered saline (PBS) with 3mg/ml bovine serum albumin (BSA) for 1 hour at room temperature and incubated with primary antibody for 1-2 hours at room temperature (or overnight at 4°C). Tissue sections were washed (4 times for 10 minutes each) in PBS and incubated in PBS/BSA with 10μg/ml of the appropriate fluorescein (or Cy2)-coupled secondary antibody for one hour. Skeletal muscle sections were also incubated with 50nM rhodamine-α-bungarotoxin to identify acetylcholine receptors (AChRs) at the NMJ. Anti-mouse antibodies were pre-complexed with secondary antibody prior to staining as previously described (Xia et al., 2002). For visualization of YFP, slides were not stained in the fluorescein channel and endogenous YFP was visualized instead. Slides were mounted in paraphenylenediamine to inhibit quenching of fluorescence. Staining was visualized using fluorescein-specific or rhodamine-specific optics on a Nikon E800 or a Zeiss Axiophot epifluorescence microscope or using a Zeiss LSM700 or LSM510 confocal microscope.

Immunoblotting

Organs from 6 week-old male mice were dissected and proteins extracted with denaturation buffer and quantitated as described previously for skeletal muscle(Xia et al., 2002). Protein samples of 40 μg per lane were separated by SDS-PAGE and immunoblotted as previously described(Xia et al., 2002). Densitometry was also performed as previously described(Nguyen et al., 2002).

Lectin Precipitation Studies

Mouse tissues were solubilized in buffer containing 1% NP40 and assayed for protein concentration as previously described(Xia et al., 2002). 150μg of extracted protein was incubated with *Wisteria floribunda* agglutinin (WFA) or Wheat Germ Agglutinin (WGA) overnight at 4°C. Samples were spun at 3800g for 3 minutes, washed 3 times 10 minutes in buffer, and denatured in SDS-containing buffer as before(Xia et al., 2002). WFA binding was verified by blocking with 0.3M GalNAc and WGA binding by blocking in 0.3M GlcNAc. Precipitated proteins were separated by SDS-PAGE and immunoblotted using antibodies to proteins or carbohydrates as previously described(Xia et al., 2002; Xia and Martin, 2002).

Quantification of muscle morphometry, endplate band width, neuromuscular diameter and AChR density

All NMJ and skeletal muscle measurements were done as previously described(Jayasinha et al., 2003; Nguyen et al., 2002; Xia et al., 2002). NMJ and myofiber cross-sectional area, number of AChR microaggregates, and central nuclei measurements were carried out using Zeiss AxioVision Rel.4.8 software. NMJ diameter was measured using whole mount

staining of NMJs in the diaphragm with rhodamine-α-bungarotoxin. Similar results were also observed for stained gastrocnemius muscles cut in cross-section. Endplate band length was measured in the diaphragm muscle, again using whole mount staining with rhodamine-α-bungarotoxin, as before(Xia and Martin, 2002). AChR-rich domains were measured by serially sectioning diaphragm and tibialis anterior muscles in the longitudinal axis at 20μm on a cryostat and labeling sections with rhodamine-α-bungarotoxin. Myofiber membranes were defined by phase microscopy. NMJs were also analyzed by staining serially cut 20μm longitudinal sections of tibialis anterior or diaphragm muscle with antibodies to synaptophysin and neurofilament, in addition to rhodamine-α-bungarotoxin, to assess the degree of innervation.

Infection of skeletal muscle with AAV1-CMV-Galgt1

Adeno associated virus vector, serotype 1 (AAV1), was synthesized and highly purified in the Viral Vector Core at The Research Institute at Nationwide Children's Hospital, as previously described(Martin et al., 2009). Mouse *Galgt1* cDNA was expressed in AAV1 vector using cytomegalovirus (CMV) promoter. A single gastrocnemius and/or tibialis anterior (TA) muscle was injected with 25μL (TA) or 50μL (Gastroc) of 1×10^{11} (TA) or 5×10^{11} (Gastroc) vector genomes (vg) of AAV1-CMV-*Galgt1*. All injections were done in 7-day old WT mice. The contralateral TA and/or Gastroc were mock-infected by injecting with an equivalent volume of PBS. Mice were sacrificed at 6 weeks or 12 weeks post-injection. Mock-infected and infected muscles were dissected and snap-frozen in liquid nitrogen-cooled isopentane.

Statistics

All determinations of significance were done by ANOVA with post-hoc Bonferroni analysis and/or unpaired t tests.

Acknowledgments

This work was supported by NIH grant AR049722 to PTM. The authors would like to thank Matthew Glass, Kumaran Chandrasekharan, Marybeth Camboni, Bing Xia, Kwame Hoyte, Christine Kang, Ling Guo and David Kim for technical assistance. We would like to thank Bruce Patton (Oregon Health Sciences University) for antibody to laminin α4, Jeffery Miner (Washington University) for antibody to laminin α5 and for P3ProCre*Dag1*^{loxP} mice, the Consortium for Functional Glycomics for *Galgt1*$^{-/-}$ mice, John Lowe (Genentech) for *Galgt2*$^{-/-}$ mice, Josh Sanes (Harvard University) for antibody to NCAM, Michael Ferns (UC Davis) for antibody to agrin and Palmer Taylor (UC San Diego) for antibody to acetylcholinesterase.

Abbreviations

GalNAc	N-acetylgalactosamine
GlcNAc	N-acetylglucosamine
Neu5Gc	N-glycolylneuraminic acid
Neu5Ac	N-acetylneuraminic acid
Gal	Galactose
Glc	Glucose
NMJ	Neuromuscular Junction
WFA	*Wisteria floribunda* agglutinin
WGA	Wheat Germ agglutinin
CT carbohydrate	Cytotoxic T cell carbohydrate

References

Bullens RW, O'Hanlon GM, Wagner E, Molenaar PC, Furukawa K, Plomp JJ, Willison HJ. Complex gangliosides at the neuromuscular junction are membrane receptors for autoantibodies and botulinum neurotoxin but redundant for normal synaptic function. The Journal of neuroscience : the official journal of the Society for Neuroscience. 2002; 22:6876–6884. [PubMed: 12177185]

Burgess RW, Nguyen QT, Son YJ, Lichtman JW, Sanes JR. Alternatively spliced isoforms of nerve- and muscle-derived agrin: their roles at the neuromuscular junction. Neuron. 1999; 23:33–44. [PubMed: 10402191]

Caroni P. Overexpression of growth-associated proteins in the neurons of adult transgenic mice. J Neurosci Methods. 1997; 71:3–9. [PubMed: 9125370]

Cohn RD, Henry MD, Michele DE, Barresi R, Saito F, Moore SA, Flanagan JD, Skwarchuk MW, Robbins ME, Mendell JR, Williamson RA, Campbell KP. Disruption of DAG1 in differentiated skeletal muscle reveals a role for dystroglycan in muscle regeneration. Cell. 2002; 110:639–648. [PubMed: 12230980]

Conzelmann A, Lefrancois L. Monoclonal antibodies specific for T cell-associated carbohydrate determinants react with human blood group antigens CAD and SDA. J Exp Med. 1988; 167:119–131. [PubMed: 2447219]

Cote PD, Moukhles H, Lindenbaum M, Carbonetto S. Chimaeric mice deficient in dystroglycans develop muscular dystrophy and have disrupted myoneural synapses. Nat Genet. 1999; 23:338–342. [PubMed: 10610181]

Covault J, Sanes JR. Distribution of N-CAM in synaptic and extrasynaptic portions of developing and adult skeletal muscle. J Cell Biol. 1986; 102:716–730. [PubMed: 3512581]

Cremer H, Lange R, Christoph A, Plomann M, Vopper G, Roes J, Brown R, Baldwin S, Kraemer P, Scheff S, et al. Inactivation of the N-CAM gene in mice results in size reduction of the olfactory bulb and deficits in spatial learning. Nature. 1994; 367:455–459. [PubMed: 8107803]

Dani N, Broadie K. Glycosylated synaptomatrix regulation of trans-synaptic signaling. Developmental neurobiology. 2012; 72:2–21. [PubMed: 21509945]

Feng G, Mellor RH, Bernstein M, Keller-Peck C, Nguyen QT, Wallace M, Nerbonne JM, Lichtman JW, Sanes JR. Imaging neuronal subsets in transgenic mice expressing multiple spectral variants of GFP. Neuron. 2000; 28:41–51. [PubMed: 11086982]

Gautam M, Noakes PG, Moscoso L, Rupp F, Scheller RH, Merlie JP, Sanes JR. Defective neuromuscular synaptogenesis in agrin-deficient mutant mice. Cell. 1996; 85:525–535. [PubMed: 8653788]

Hoyte K, Kang C, Martin PT. Definition of pre- and postsynaptic forms of the CT carbohydrate antigen at the neuromuscular junction: ubiquitous expression of the CT antigens and the CT GalNAc transferase in mouse tissues. Brain Res Mol Brain Res. 2002; 109:146–160. [PubMed: 12531524]

Jarad G, Miner JH. The Pax3-Cre transgene exhibits a rostrocaudal gradient of expression in the skeletal muscle lineage. Genesis. 2009; 47:1–6. [PubMed: 18942111]

Jayasinha V, Nguyen HH, Xia B, Kammesheidt A, Hoyte K, Martin PT. Inhibition of dystroglycan cleavage causes muscular dystrophy in transgenic mice. Neuromuscul Disord. 2003; 13:365–375. [PubMed: 12798792]

Jenniskens GJ, Oosterhof A, Brandwijk R, Veerkamp JH, van Kuppevelt TH. Heparan sulfate heterogeneity in skeletal muscle basal lamina: demonstration by phage display-derived antibodies. J Neurosci. 2000; 20:4099–4111. [PubMed: 10818145]

Kawamura YI, Kawashima R, Fukunaga R, Hirai K, Toyama-Sorimachi N, Tokuhara M, Shimizu T, Dohi T. Introduction of Sd(a) carbohydrate antigen in gastrointestinal cancer cells eliminates selectin ligands and inhibits metastasis. Cancer research. 2005; 65:6220–6227. [PubMed: 16024623]

Lefrancois L, Bevan MJ. Functional modifications of cytotoxic T-lymphocyte T200 glycoprotein recognized by monoclonal antibodies. Nature. 1985; 314:449–452. [PubMed: 2580241]

Li J, Chen F, Epstein JA. Neural crest expression of Cre recombinase directed by the proximal Pax3 promoter in transgenic mice. Genesis. 2000; 26:162–164. [PubMed: 10686619]

Martin PT. Glycobiology of the synapse. Glycobiology. 2002; 12:1R–7R. [PubMed: 11825880]

Martin PT. Dystroglycan glycosylation and its role in matrix binding in skeletal muscle. Glycobiology. 2003a; 13:55R–66R.

Martin PT. Glycobiology of the neuromuscular junction. J Neurocytol. 2003b; 32:915–929. [PubMed: 15034276]

Martin PT, Freeze HH. Glycobiology of neuromuscular disorders. Glycobiology. 2003; 13:67R–75R.

Martin PT, Scott LJ, Porter BE, Sanes JR. Distinct structures and functions of related pre- and postsynaptic carbohydrates at the mammalian neuromuscular junction. Mol Cell Neurosci. 1999; 13:105–118. [PubMed: 10192769]

Martin PT, Xu R, Rodino-Klapac LR, Oglesbay E, Camboni M, Montgomery CL, Shontz K, Chicoine LG, Clark KR, Sahenk Z, Mendell JR, Janssen PM. Overexpression of Galgt2 in skeletal muscle prevents injury resulting from eccentric contractions in both mdx and wild-type mice. Am J Physiol Cell Physiol. 2009; 296:C476–488. [PubMed: 19109526]

Matsumura K, Ervasti JM, Ohlendieck K, Kahl SD, Campbell KP. Association of dystrophin-related protein with dystrophin-associated proteins in mdx mouse muscle. Nature. 1992; 360:588–591. [PubMed: 1461282]

Misgeld T, Kummer TT, Lichtman JW, Sanes JR. Agrin promotes synaptic differentiation by counteracting an inhibitory effect of neurotransmitter. Proc Natl Acad Sci U S A. 2005; 102:11088–11093. [PubMed: 16043708]

Montiel MD, Krzewinski-Recchi MA, Delannoy P, Harduin-Lepers A. Molecular cloning, gene organization and expression of the human UDP-GalNAc:Neu5Acalpha2-3Galbeta-R beta1,4-N-acetylgalactosaminyltransferase responsible for the biosynthesis of the blood group Sda/Cad antigen: evidence for an unusual extended cytoplasmic domain. Biochem J. 2003; 373:369–379. [PubMed: 12678917]

Moore SA, Saito F, Chen J, Michele DE, Henry MD, Messing A, Cohn RD, Ross-Barta SE, Westra S, Williamson RA, Hoshi T, Campbell KP. Deletion of brain dystroglycan recapitulates aspects of congenital muscular dystrophy. Nature. 2002; 418:422–425. [PubMed: 12140559]

Mukasa R, Umeda M, Endo T, Kobata A, Inoue K. Characterization of glycosylphosphatidylinositol (GPI)-anchored NCAM on mouse skeletal muscle cell line C2C12: the structure of the GPI glycan and release during myogenesis. Arch Biochem Biophys. 1995; 318:182–190. [PubMed: 7726560]

Nguyen HH, Jayasinha V, Xia B, Hoyte K, Martin PT. Overexpression of the cytotoxic T cell GalNAc transferase in skeletal muscle inhibits muscular dystrophy in mdx mice. Proc Natl Acad Sci U S A. 2002; 99:5616–5621. [PubMed: 11960016]

Nishimune H, Valdez G, Jarad G, Moulson CL, Muller U, Miner JH, Sanes JR. Laminins promote postsynaptic maturation by an autocrine mechanism at the neuromuscular junction. J Cell Biol. 2008; 182:1201–1215. [PubMed: 18794334]

Pan B, Fromholt SE, Hess EJ, Crawford TO, Griffin JW, Sheikh KA, Schnaar RL. Myelin-associated glycoprotein and complementary axonal ligands, gangliosides, mediate axon stability in the CNS and PNS: neuropathology and behavioral deficits in single- and double-null mice. Exp Neurol. 2005; 195:208–217. [PubMed: 15953602]

Rushton E, Rohrbough J, Deutsch K, Broadie K. Structure-function analysis of endogenous lectin mind-the-gap in synaptogenesis. Developmental neurobiology. 2012

Rutishauser U, Landmesser L. Polysialic acid in the vertebrate nervous system: a promoter of plasticity in cell-cell interactions. Trends Neurosci. 1996; 19:422–427. [PubMed: 8888519]

Sanes JR, Cheney JM. Lectin binding reveals a synapse-specific carbohydrate in skeletal muscle. Nature. 1982; 300:646–647. [PubMed: 7144916]

Sanes JR, Lichtman JW. Induction, assembly, maturation and maintenance of a postsynaptic apparatus. Nat Rev Neurosci. 2001; 2:791–805. [PubMed: 11715056]

Scott LJ, Bacou F, Sanes JR. A synapse-specific carbohydrate at the neuromuscular junction: association with both acetylcholinesterase and a glycolipid. J Neurosci. 1988; 8:932–944. [PubMed: 3346730]

Sheikh KA, Sun J, Liu Y, Kawai H, Crawford TO, Proia RL, Griffin JW, Schnaar RL. Mice lacking complex gangliosides develop Wallerian degeneration and myelination defects. Proc Natl Acad Sci U S A. 1999; 96:7532–7537. [PubMed: 10377449]

Singhal N, Martin PT. Role of extracellular matrix proteins and their receptors in the development of the vertebrate neuromuscular junction. Developmental neurobiology. 2011; 71:982–1005. [PubMed: 21766463]

Smith PL, Lowe JB. Molecular cloning of a murine N-acetylgalactosamine transferase cDNA that determines expression of the T lymphocyte-specific CT oligosaccharide differentiation antigen. J Biol Chem. 1994; 269:15162–15171. [PubMed: 7515051]

Takamiya K, Yamamoto A, Furukawa K, Yamashiro S, Shin M, Okada M, Fukumoto S, Haraguchi M, Takeda N, Fujimura K, Sakae M, Kishikawa M, Shiku H, Aizawa S. Mice with disrupted GM2/GD2 synthase gene lack complex gangliosides but exhibit only subtle defects in their nervous system. Proc Natl Acad Sci U S A. 1996; 93:10662–10667. [PubMed: 8855236]

Varki A. Nothing in glycobiology makes sense, except in the light of evolution. Cell. 2006; 126:841–845. [PubMed: 16959563]

Walsh FS, Hobbs C, Wells DJ, Slater CR, Fazeli S. Ectopic expression of NCAM in skeletal muscle of transgenic mice results in terminal sprouting at the neuromuscular junction and altered structure but not function. Mol Cell Neurosci. 2000; 15:244–261. [PubMed: 10736202]

Williamson RA, Henry MD, Daniels KJ, Hrstka RF, Lee JC, Sunada Y, Ibraghimov-Beskrovnaya O, Campbell KP. Dystroglycan is essential for early embryonic development: disruption of Reichert's membrane in Dag1-null mice. Hum Mol Genet. 1997; 6:831–841. [PubMed: 9175728]

Xia B, Hoyte K, Kammesheidt A, Deerinck T, Ellisman M, Martin PT. Overexpression of the CT GalNAc transferase in skeletal muscle alters myofiber growth, neuromuscular structure, and laminin expression. Dev Biol. 2002; 242:58–73. [PubMed: 11795940]

Xia B, Martin PT. Modulation of agrin binding and activity by the CT and related carbohydrate antigens. Mol Cell Neurosci. 2002; 19:539–551. [PubMed: 11988021]

Xiao X, Li J, Samulski RJ. Production of high-titer recombinant adeno-associated virus vectors in the absence of helper adenovirus. J Virol. 1998; 72:2224–2232. [PubMed: 9499080]

Xu R, Chandrasekharan K, Yoon JH, Camboni M, Martin PT. Overexpression of the cytotoxic T cell (CT) carbohydrate inhibits muscular dystrophy in the dyW mouse model of congenital muscular dystrophy 1A. Am J Pathol. 2007; 171:181–199. [PubMed: 17591965]

Xu R, DeVries S, Camboni M, Martin PT. Overexpression of Galgt2 reduces dystrophic pathology in the skeletal muscles of alpha sarcoglycan-deficient mice. Am J Pathol. 2009; 175:235–247. [PubMed: 19498002]

Yoon JH, Chandrasekharan K, Xu R, Glass M, Singhal N, Martin PT. The synaptic CT carbohydrate modulates binding and expression of extracellular matrix proteins in skeletal muscle: Partial dependence on utrophin. Mol Cell Neurosci. 2009; 41:448–463. [PubMed: 19442736]

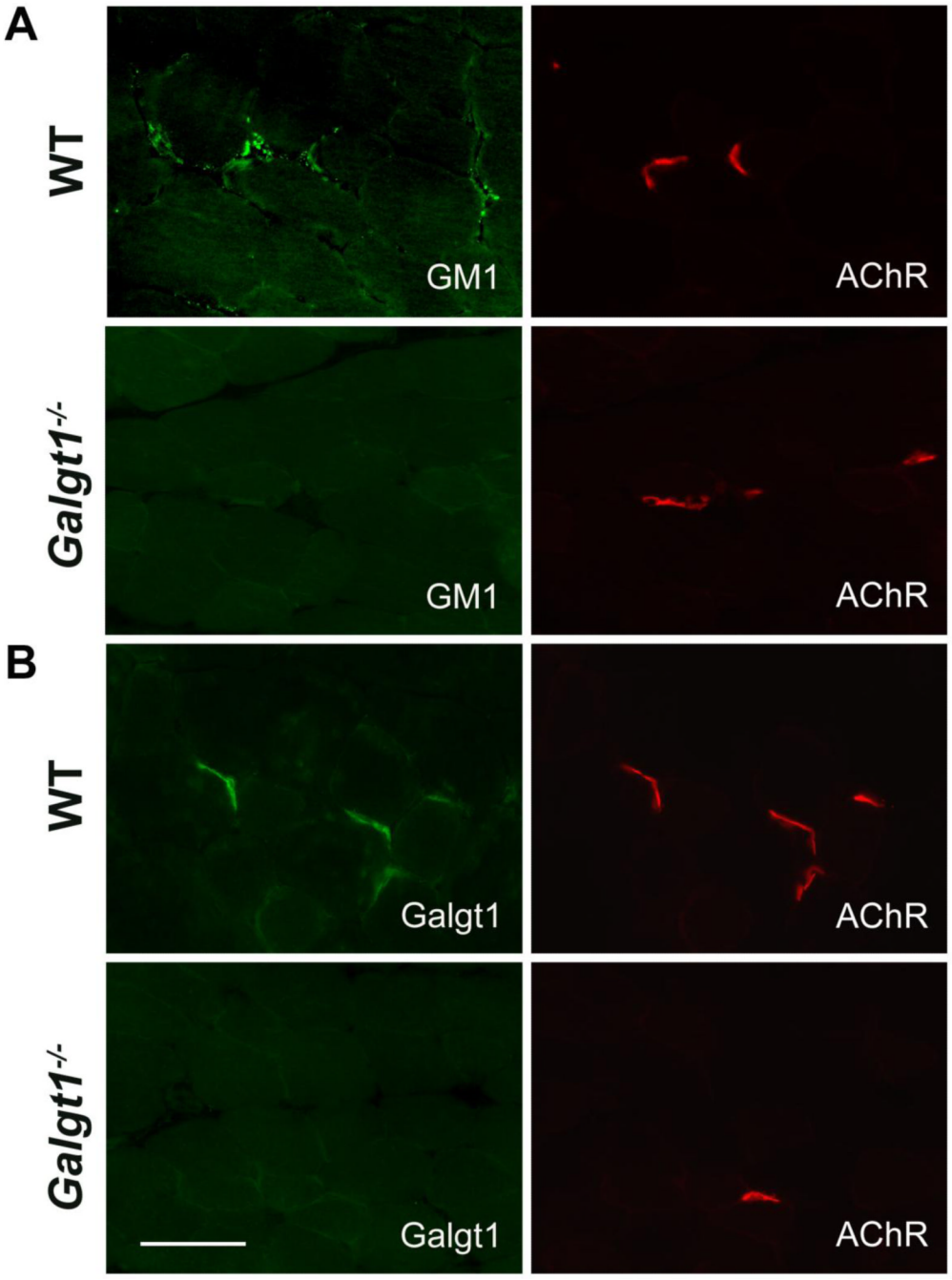

Fig. 1. Galgt1 and GM1 are expressed at the neuromuscular junction

An affinity purified antisera to GM1 (A) or Galgt1 (B) was used to immunostain wild type (WT) or *Galgt1*$^{-/-}$ mouse skeletal muscle (Gastroc), which was co-stained with rhodamine-α-bungarotoxin to label nicotinic acetylcholine receptors (AChR) concentrated at the neuromuscular junction (NMJ). Bar is 50μm for all panels.

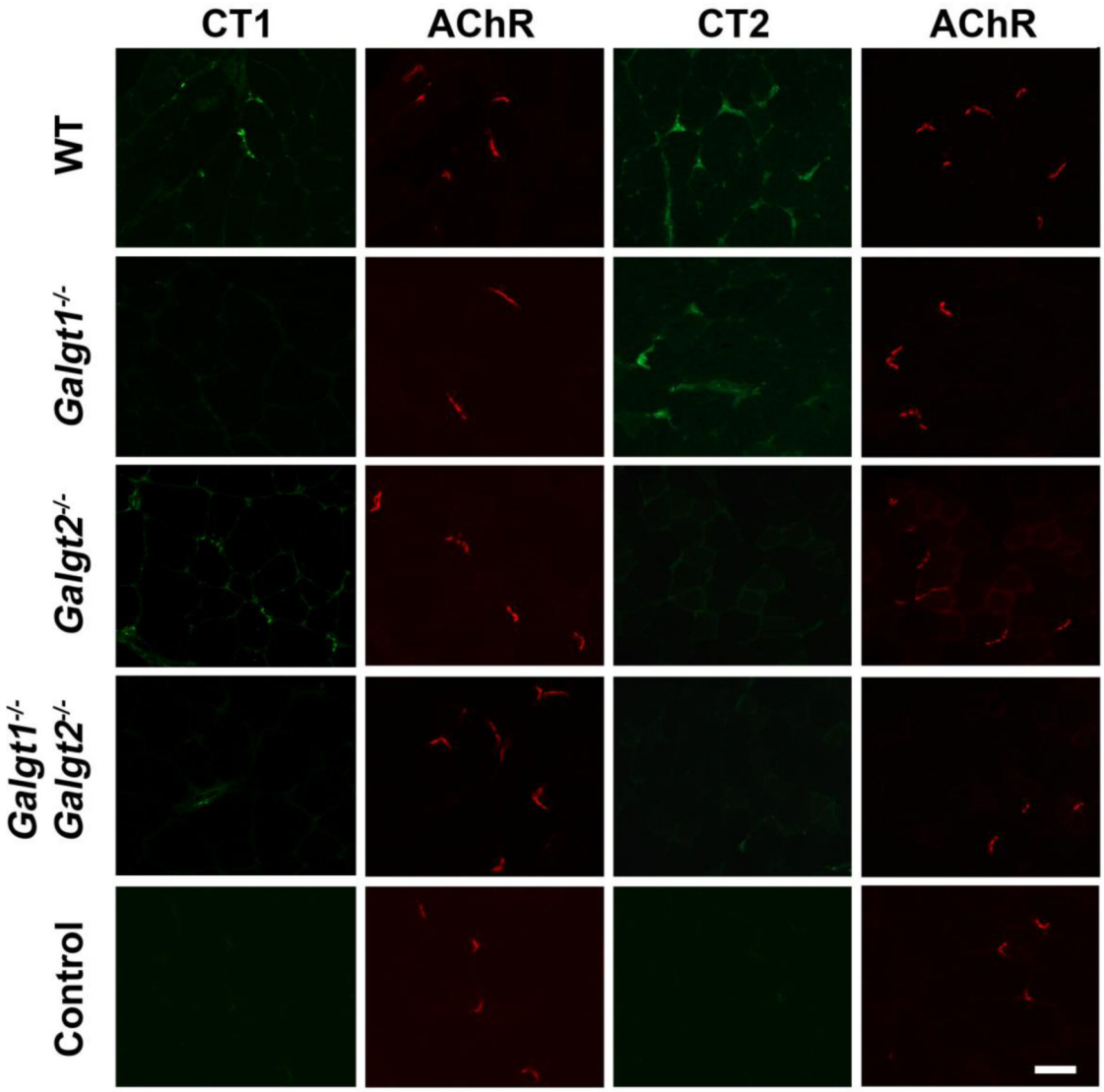

Fig. 2. *Galgt1* and *Galgt2* differentially contribute to expression of the CT carbohydrate at the neuromuscular junction

Skeletal muscle (Tibialis anterior) from 6 week-old wild type (WT), *Galgt1*$^{-/-}$, *Galgt2*$^{-/-}$, and *Galgt1*$^{-/-}$*Galgt2*$^{-/-}$ was stained with CT1, CT2, or secondary antibody only (Control) and with rhodamine-α-bungarotoxin, to label acetylcholine receptors (AChR) at the NMJ. Bar is 20μm for all panels.

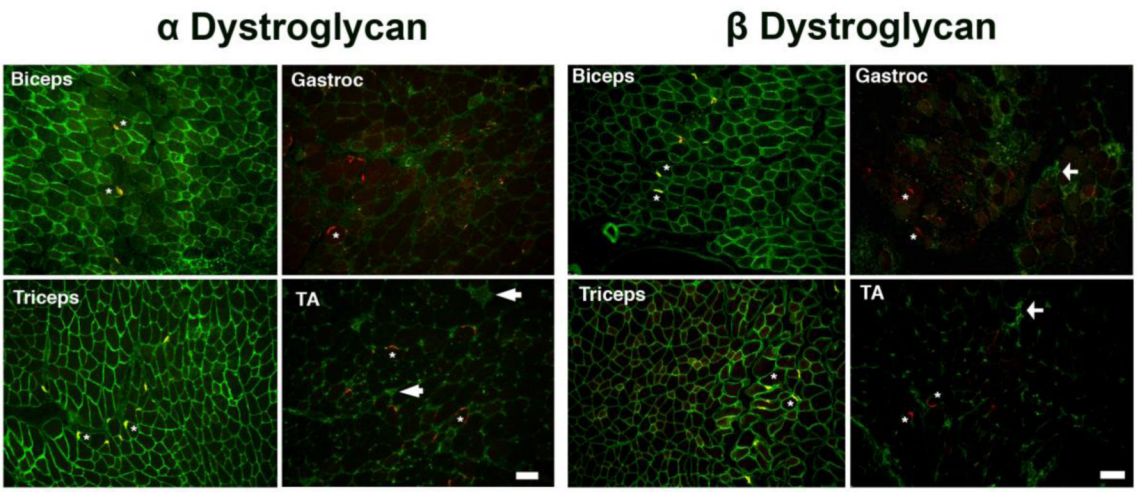

Fig. 3. Deletion of dystroglycan expression in P3ProCre*Dag1*$^{loxP/loxP}$ hindlimb muscles

Skeletal muscles from P3Pro-Cre*Dag1*$^{loxP/loxP}$ mice were co-stained with an antibody to α dystroglycan or β dystroglycan (green) and rhodamine-α-bungarotoxin (red) to label AChRs at the NMJ. Merged images are shown, with overlap as yellow. Some NMJs are marked with an asterisk. Some mononuclear cells expressing α and β dystroglycan in dystrophic *Dag1*-deleted muscles are marked with an arrow. Bar is 50μm for all panels. TA, Tibialis anterior

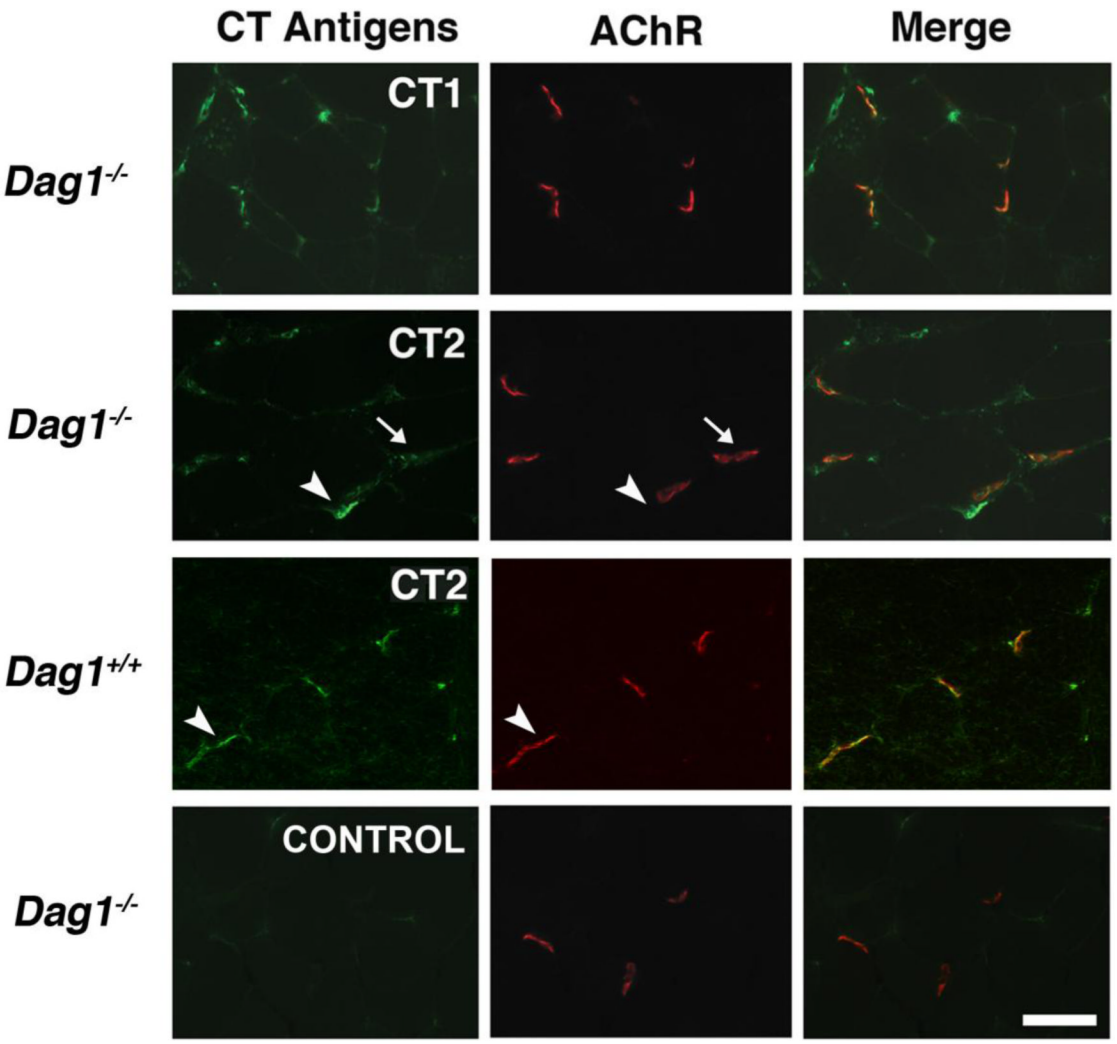

Fig. 4. Synaptic expression of the CT2 carbohydrate is altered in *Dag1*$^{-/-}$ muscle

Skeletal muscle from 8 week-old P3ProCre*Dag1*$^{loxP/loxP}$ (*Dag1*$^{-/-}$) or wild type (*Dag1*$^{+/+}$) mice were stained with CT1, CT2 or secondary antibody alone (Control) and co-stained with rhodamine-α-bungarotoxin to label acetylcholine receptors (AChR) at the NMJ. Arrowheads mark the CT2 staining either offset from the NMJ (*Dag1*$^{-/-}$) or co-localized with the NMJ (*Dag1*$^{+/+}$). Diminished CT2 staining at the NMJ in *Dag1*$^{-/-}$ muscle is marked by an arrow. Bar is 25μm for all panels.

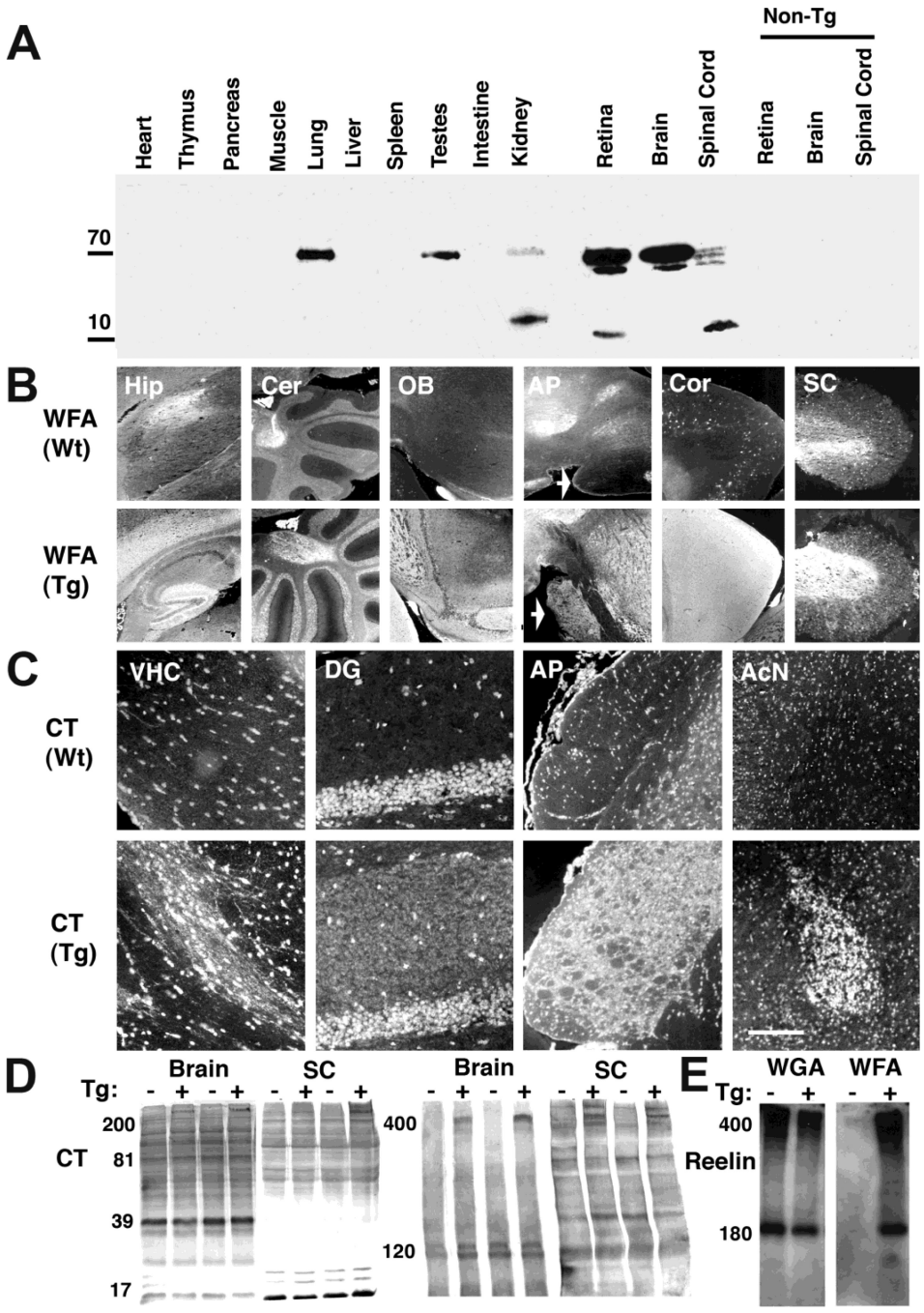

Fig. 5. Creation of transgenic mice overexpressing *Galgt2* in neurons

Transgenic mice were made to overexpress the CT GalNAc transferase (*Galgt2*) cDNA in neurons using the Thy-1.2 promoter cassette. Anti-FLAG immunoblot of FLAG-tagged Galgt2 transgenic protein expression (A). Staining with the ßGalNAc binding lectin WFA in brain and spinal cord in wild type (Wt) and *Galgt2* transgenic (Tg) animals (B, arrow shows AP). Immunostaining for CT carbohydrate antibody (CT1) in Wt and Tg brain (C). Immunoblot of CT carbohydrate (CT1) in wild type (-) and Tg (+) brain and spinal cord (D). The blot was split to allow better resolution of proteins of different sizes. Anti-Reelin immunoblot of WGA- and WFA-precipitated Wt(-) and Tg (+) brain protein (E). Hippocampus (Hip), Cerebellum (Cer), Olfactory bulb (OB), Anterior pituitary (AP), Cortex

(Cor), Spinal cord (SC), Ventral hippocampal commissure (VHC), Dentate gyrus (DG), Accumbens nucleus (AcN). Bar is 5mm for all panels in B and 500μm for panels in C.

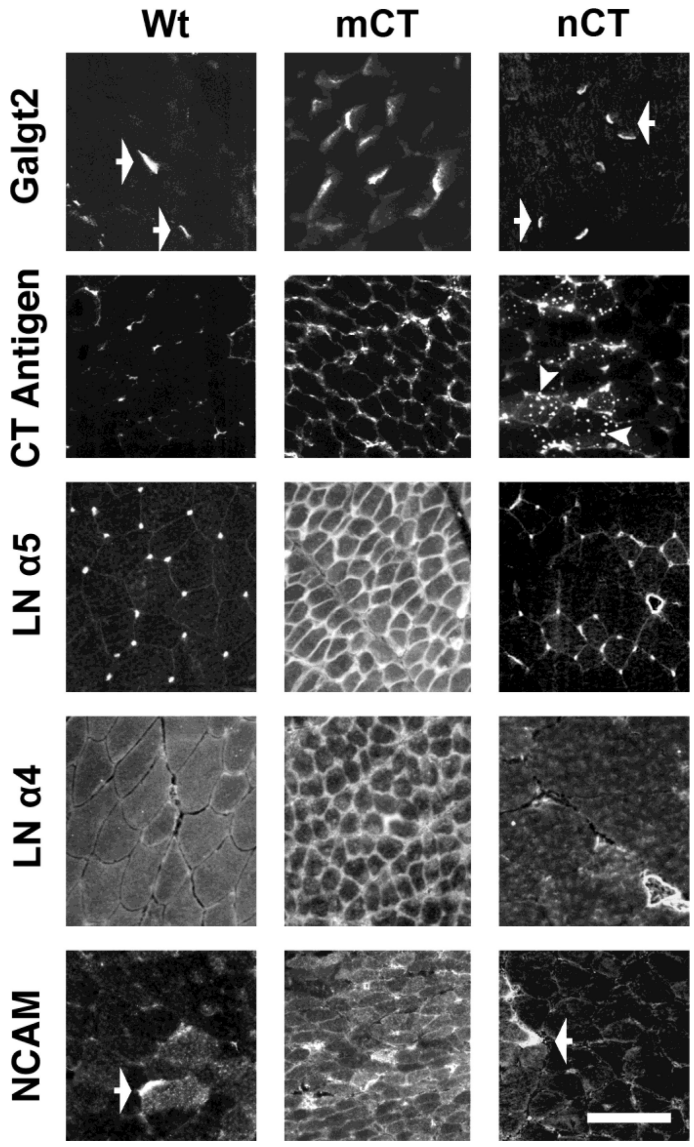

Fig. 6. Expression of neuromuscular proteins in muscle-specific and neuron-specific *Galgt2* in transgenic mice

Comparison of expression of CT GalNAc transferase (Galgt2), CT carbohydrate antigen, laminin α5 (LNα5), laminin α4 (LNα4), and neural cell adhesion molecules (NCAM) in wild type (Wt), muscle-specific *Galgt2* transgenic (mCT) and neuron-specific *Galgt2* transgenic (nCT) skeletal muscle (Gastroc). Some NMJs are marked with arrows and some intracellular accumulations of CT antigen are marked with arrowheads. Bar is 50 μm for all panels.

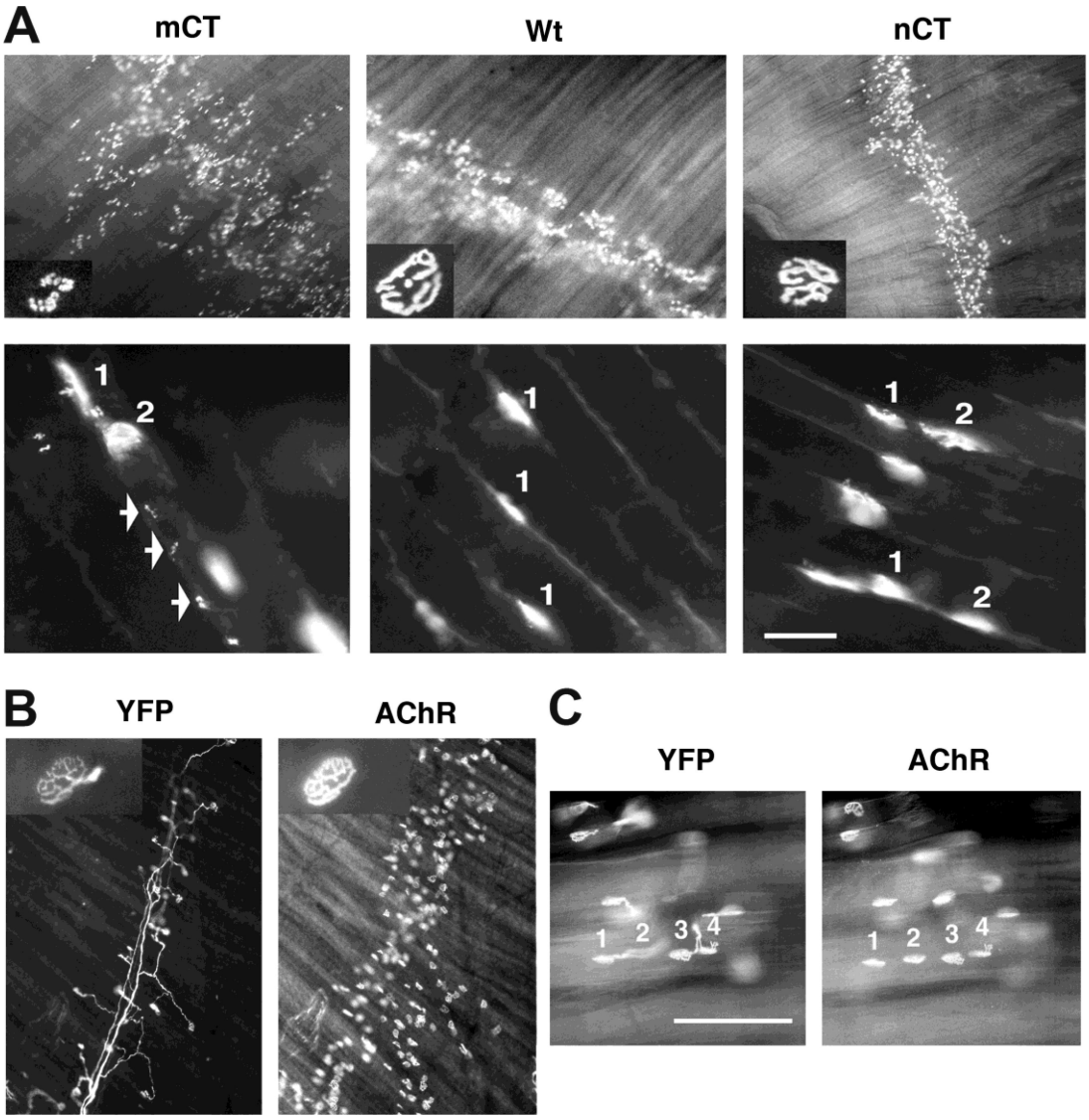

Fig. 7. Comparison of neuromuscular development in muscle-specific and neuron-specific *Galgt2* in transgenic mice

(A) Diaphragm muscle from muscle-specific (mCT) and neuron-specific (nCT) *Galgt2* transgenic mice and non-transgenic wild type (Wt) mice was stained with rhodamine-α-bungarotoxin to label acetylcholine receptors (AChRs) at the NMJ (upper panels). Staining of representative NMJ is shown in the insert. Lower panels show longitudinal sections of skeletal muscle stained with rhodamine-α-bungarotoxin. Multiple NMJs along single myofibers are numbered. Small AChR microaggregates are labeled by arrows. Bar is 20 μm for lower panels, 500 μm for upper panels and 20 μm for inserts. (B) Whole mount staining of the diaphragm from nCT/YFP-H double transgenic mice with rhodamine-α-bungarotoxin. Bar in A represents 20 μm for insert and 200 μm for lower panels. (C) Teased skeletal myofibers from nCT/YFP-H mice stained with rhodamine-α-bungarotoxin. Multiple NMJs along single myofibers are numbered. Bar is 200μm.

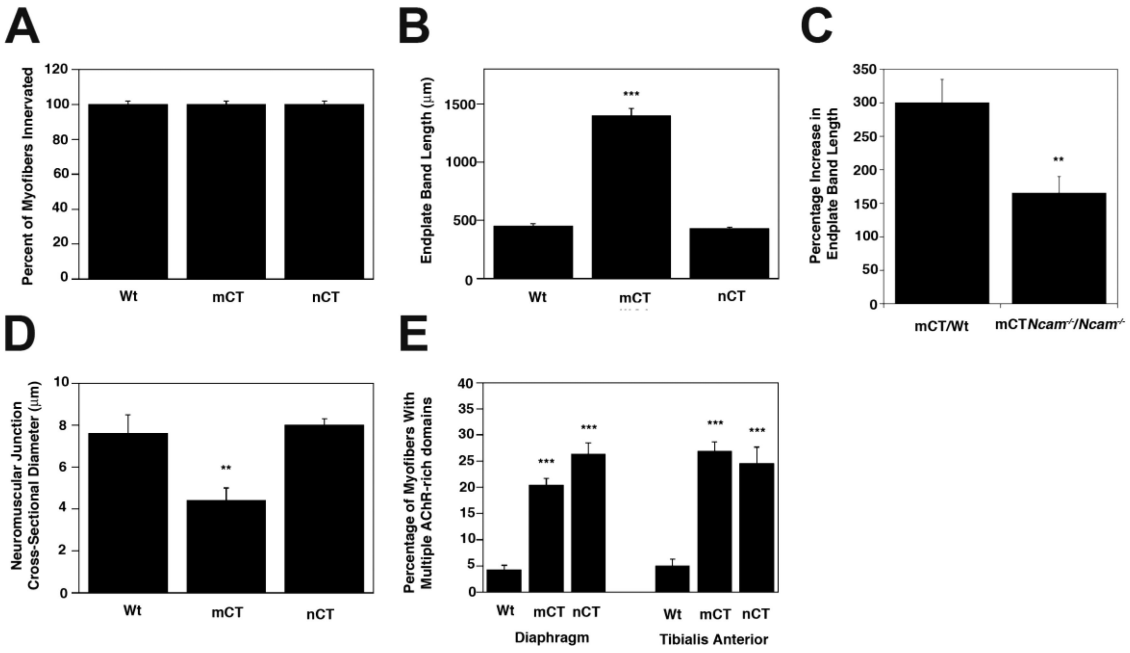

Fig. 8. Quantification of changed neuromuscular development in mCT and nCT mice

Quantification of percent innervation (A) and endplate band length (B) in wild type (Wt), muscle-specific (mCT) and neuron-specific (nCT) *Galgt2* transgenic muscle (diaphragm). Comparison of endplate band length in the diaphragm of mCT mice, relative to Wt, in the presence or absence of NCAM (C). Quantification of NMJ cross-sectional diameter (D) and percentage of myofibers with multiple AChR-rich postsynaptic domains (E) in wild type (Wt), mCT and nCT mice. n=160 synapses per condition in A, 20 muscles per condition in B and C, 12 muscles per condition in D and 160 synapses per condition in E. All errors are SEM. *P<0.05, **P<0.01, ***P<0.001

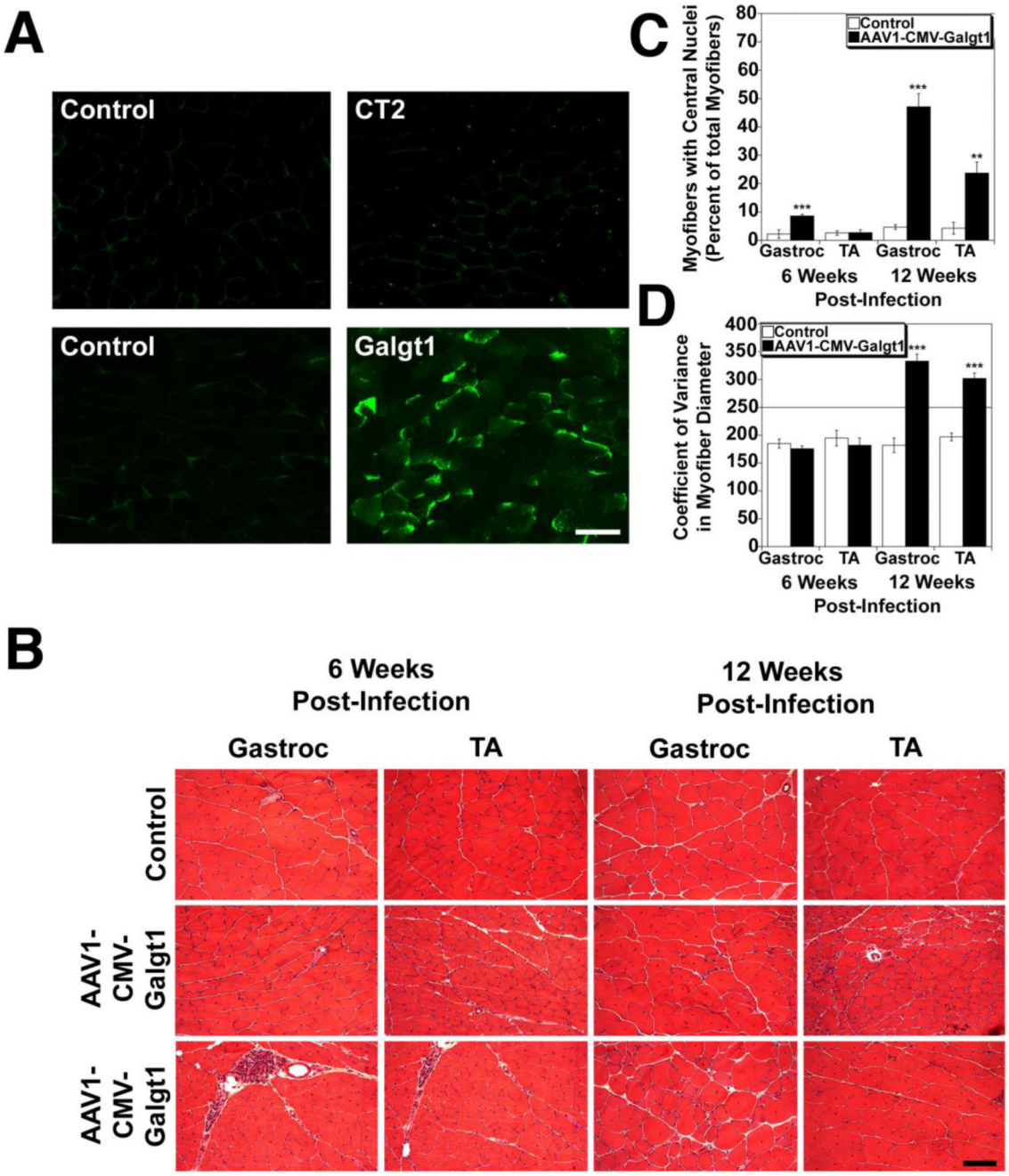

Fig. 9. *Galgt1* overexpression in skeletal myofibers fails to induce membrane expression of CT carbohydrate and causes myopathic changes

(A) Galgt1 protein and CT carbohydrate immunostaining (CT2) of an AAV1-CMV-*Galgt1*-infected wild type muscle at 6 weeks post-infection. Bar is 50μm for all panels. (B) Hematoxylin and eosin staining of cross-sections of Gastrocnemius (Gastroc) and Tibialis anterior (TA) muscles at 6 weeks or 12 weeks post-infection with AAV1-CMV-*Galgt1* compared to mock-infected contralateral controls. Bar is 50μm for all panels. (C) Quantification of the percentage of myofibers with centrally located nuclei in AAV1-CMV-*Galgt1*-infected muscles and mock-infected contralateral controls. n=6-15 muscles per condition. (D) Quantification of the variance in myofiber diameter. Measures below 250

(line) are considered normal, while higher measures are suggestive of dystrophy. n=6-15 muscles per condition. Errors are SEM. ***P<0.001, **P<0.01

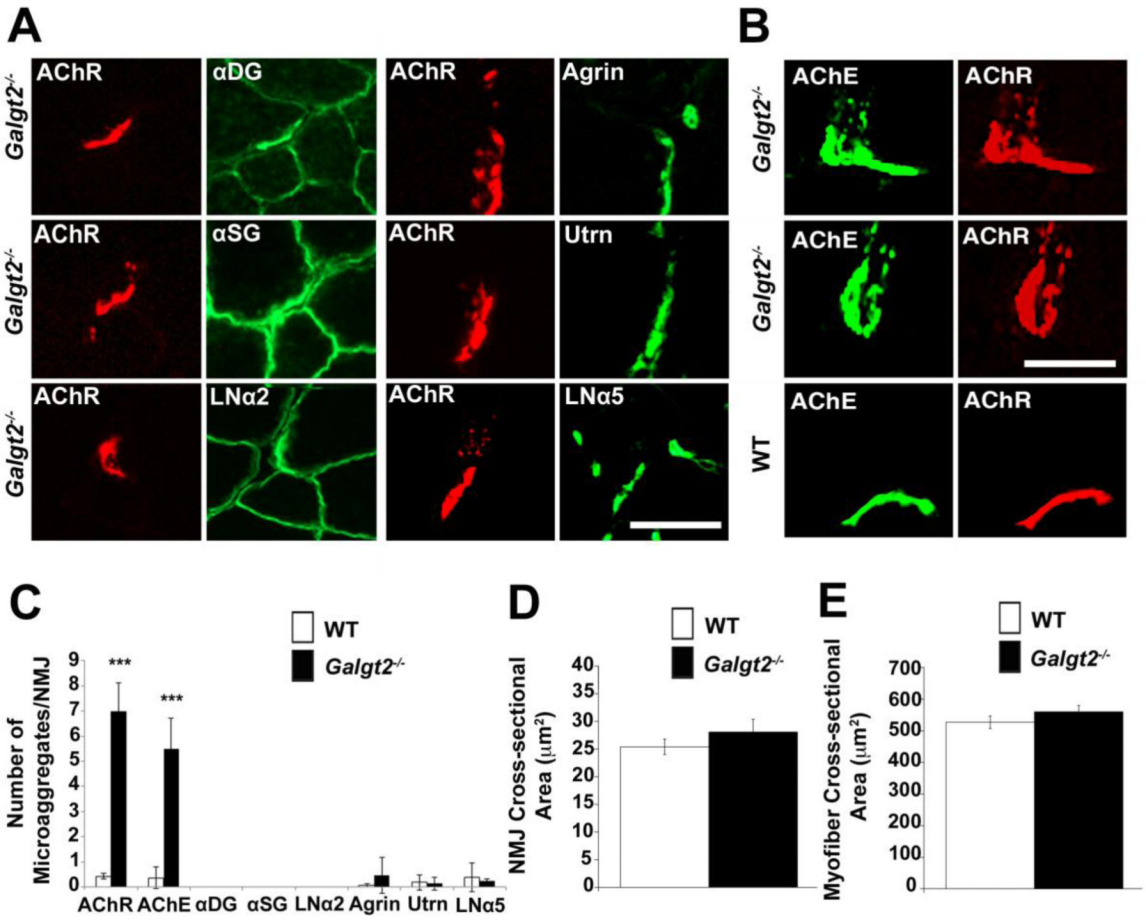

Fig. 10. Neuromuscular phenotype in *Galgt2*$^{-/-}$ muscle

(A) *Galgt2*$^{-/-}$ skeletal muscle cross-sections were immunostained with antibodies to α dystroglycan (αDG), α sarcoglycan (αSG), laminin α2 (LNα2), agrin, utrophin (Utrn) or laminin α5 (LNα5) (green). Sections were co-stained with rhodamine-α-bungarotoxin to label nicotinic acetylcholine receptors (AChRs) at the NMJ (red). Bar is 10μm for all panels in A and B. (B) AChRs co-stained with acetylcholinesterase (AChE) in *Galgt2*$^{-/-}$ muscles. (C) Intracellular microaggregates of muscle AChR, AChE, αDG, αSG, LNα2, agrin, Utrn, and LNα5 were quantified per NMJ in wild type (WT) and *Galgt2*$^{-/-}$ muscle at 3 months of age. Average cross-sectional area of NMJs (D) and skeletal myofibers (E) was quantified at 3 months of age. n=37-74 (*Galgt2*$^{-/-}$) or 46-71 (WT) synapses per condition in C and D and n=110 (*Galgt2*$^{-/-}$) or 140 (WT) myofibers per condition in E for at least 6 animals per measure. Errors are SEM for all figures. ***P<0.001 (WT vs. *Galgt2*$^{-/-}$)

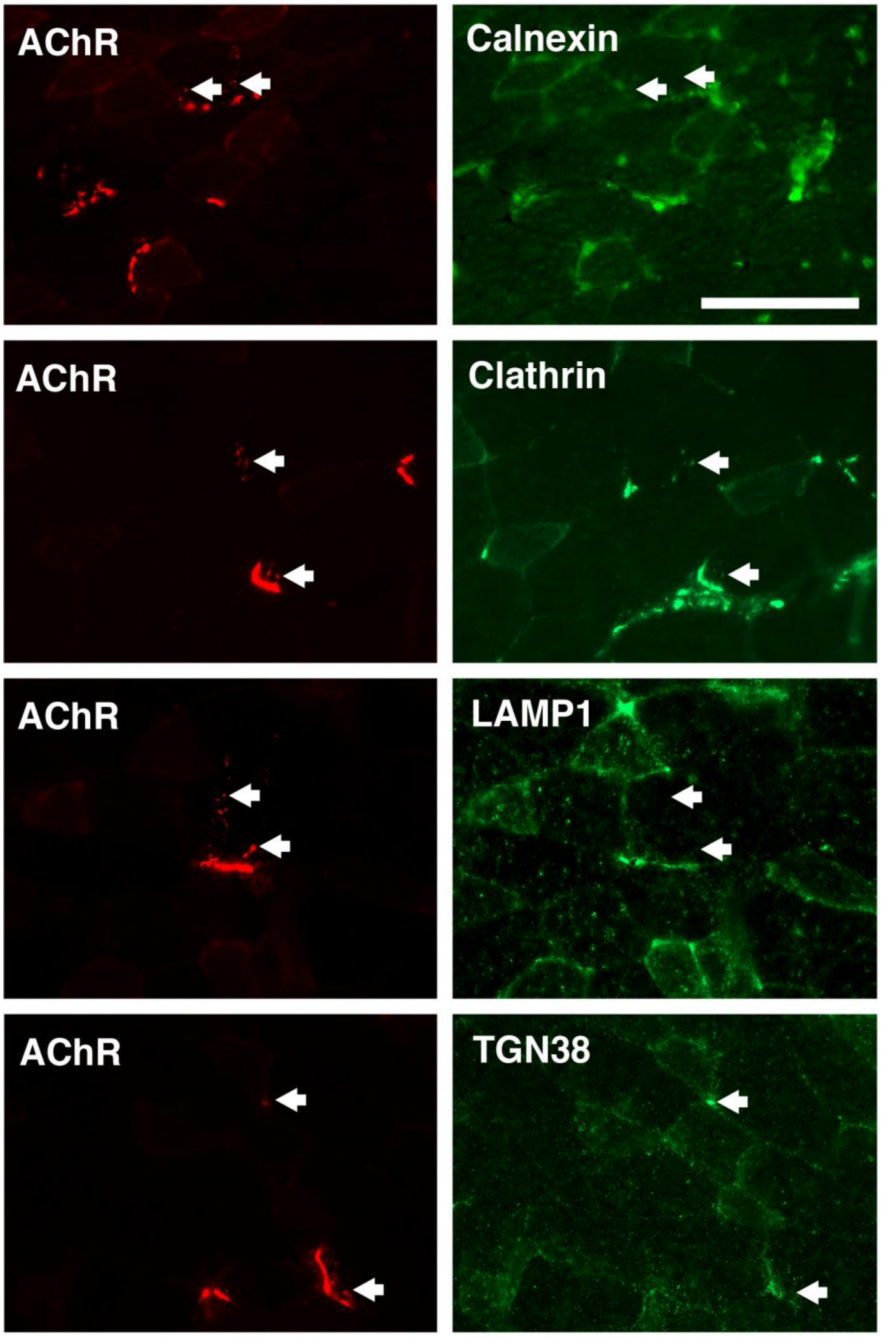

Fig. 11. Co-localization of intracellular AChR microaggregates with an endosomal marker in *Galgt2*$^{-/-}$ muscle

Skeletal muscle cross-sections from 3 month-old *Galgt2*$^{-/-}$ animals were co-stained with calnexin, clathrin heavy chain, LAMP1, or TGN38 and rhodamine-α-bungarotoxin to label AChRs. Arrows mark representative regions of α bugarotoxin-positive AChR microaggregates in both panels. Bar is 50μm for all panels.